# Consensus statement on thoracic radiology terminology in Portuguese used in Brazil and in Portugal

Bruno Hochhegger[1,2,3], Edson Marchiori[4], Rosana Rodrigues[5],
Alexandre Mançano[6], Dany Jasinowodolinski[4], Rodrigo Caruso Chate[7],
Arthur Soares Souza Jr[8], Alexandre Marchini Silva[9], Márcio Sawamura[10],
Marcelo Furnari[6], Cesar Araujo-Neto[11], Dante Escuissato[12], Rogerio Pinetti[13],
Luiz Felipe Nobre[14], Danny Warszawiak[15], Gilberto Szarf[16],
Gustavo Borges da Silva Telles[7], Gustavo Meirelles[17], Pablo Rydz Santana[18],
Viviane Antunes[13], Julia Capobianco[19], Israel Missrie[19],
Luciana Volpon Soares Souza[8], Marcel Koenigkam Santos[20], Klaus Irion[21],
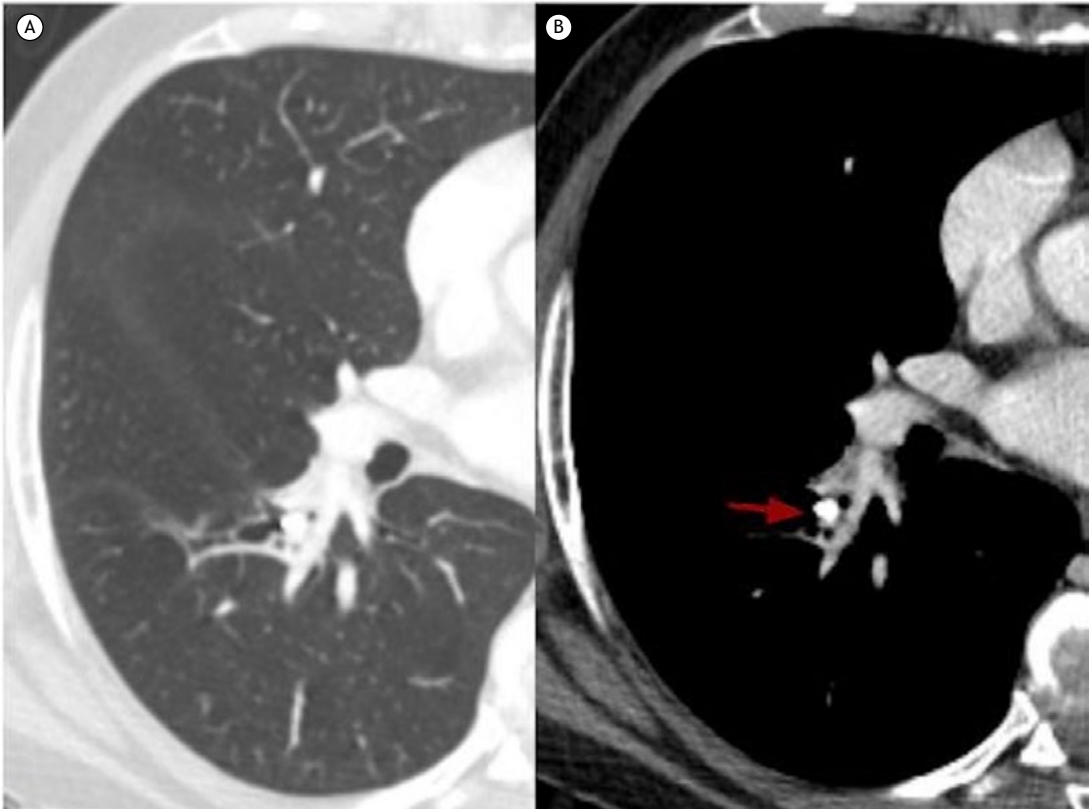Isabel Duarte[22], Rosana Santos[23], Erique Pinto[23], Diana Penha[23]
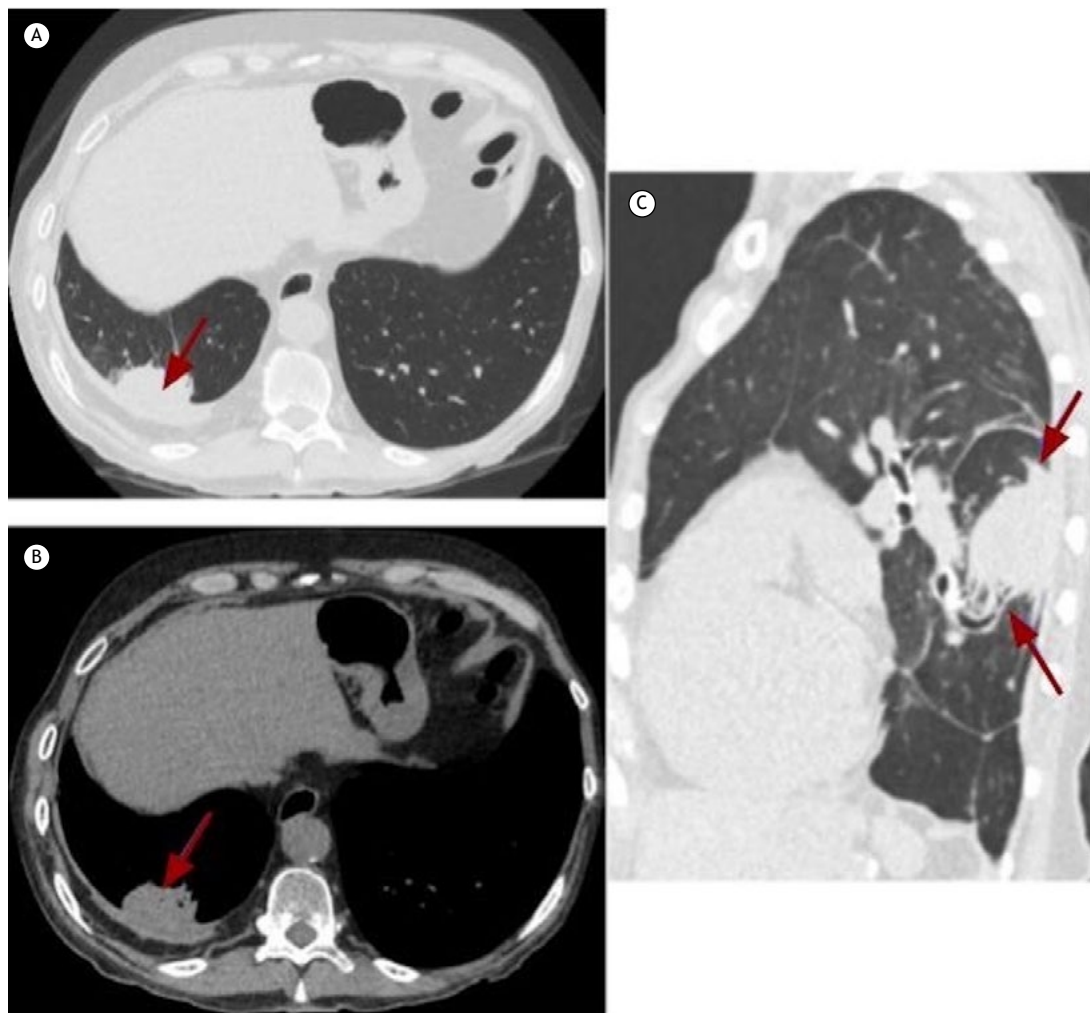
**Figure S1.** Axial CT scans with lung (A) and mediastinal window (B) settings showing a rounded opacity at the posterior right lung base, associated with pleural thickening and hypertrophy of the adjacent pleural fat (arrow). In C, sagittal plane reconstruction (lung window setting) demonstrating a rounded opacity in the left lower lobe, abutting the posterior pleural surface, associated with a curvilinear appearance of the vascular and bronchial structures in the lesion margins (arrows).
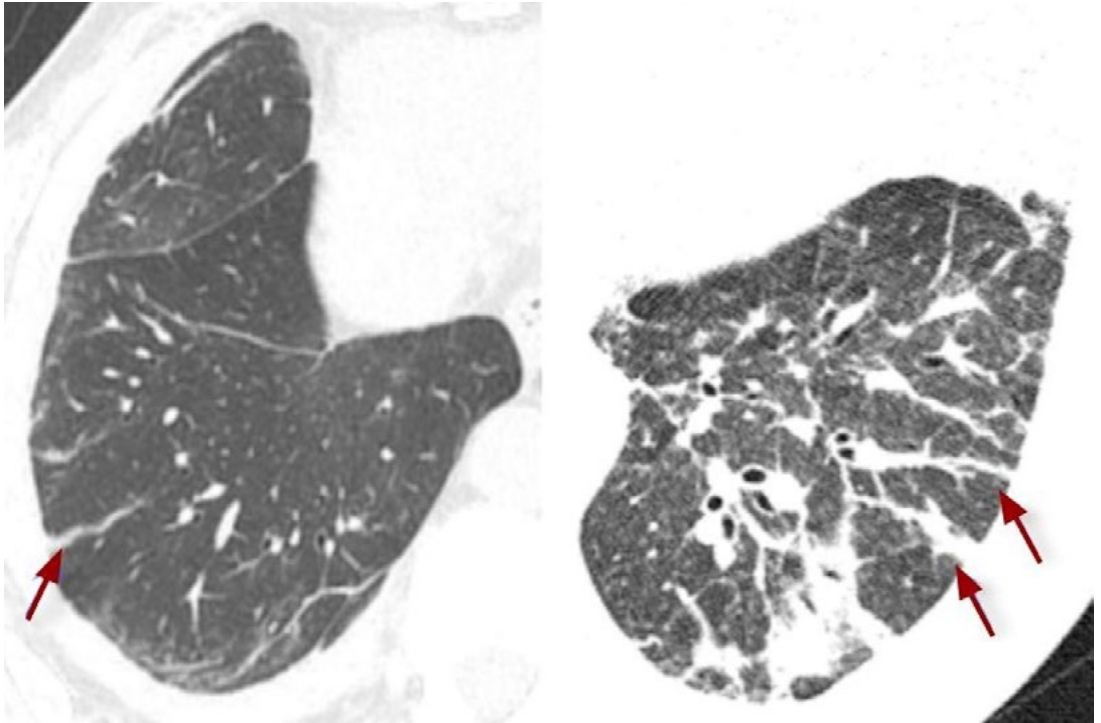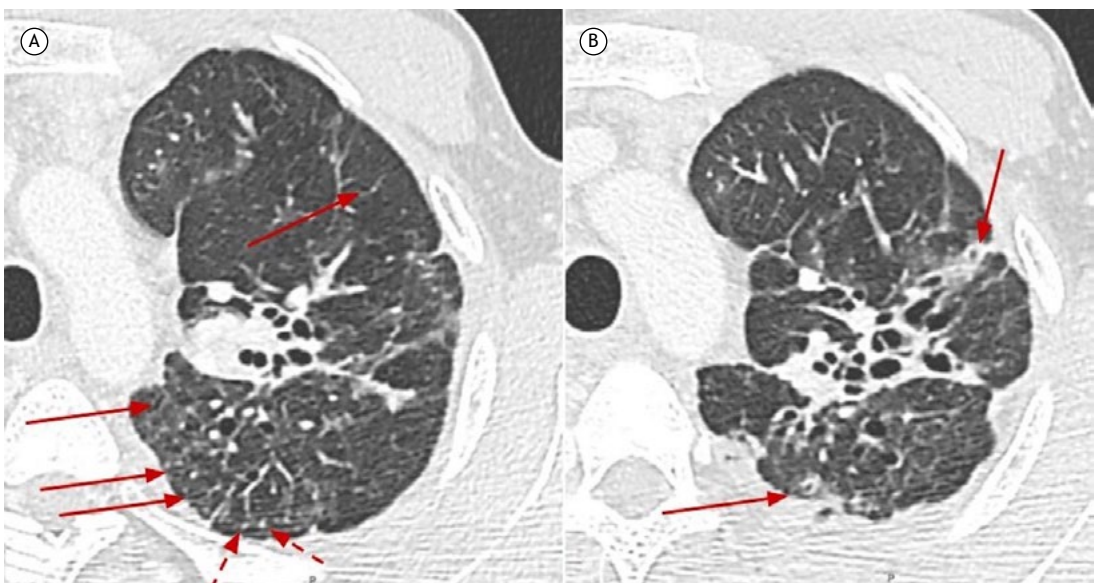
**Figure S2.** Axial CT scans with lung window settings showing several basal parenchymal bands (arrows) in two different male patients with a history of asbestos exposure.
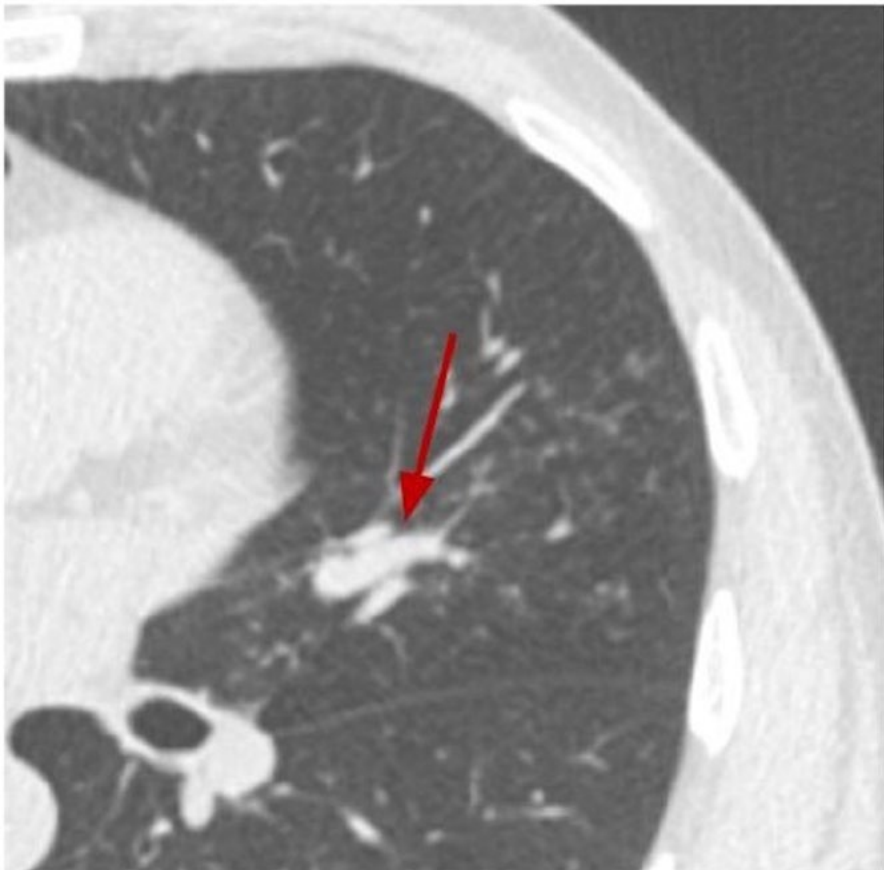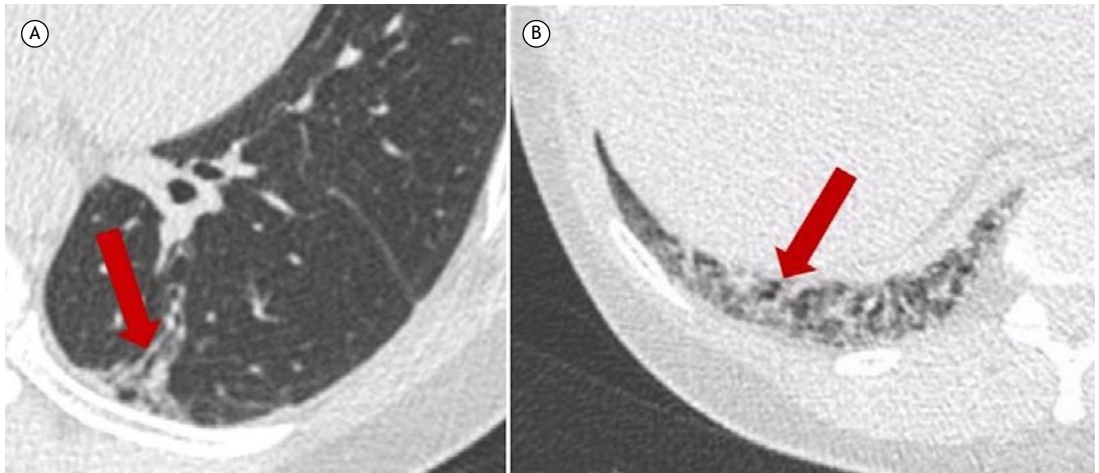


**Figure S3.** An axial CT scan with lung window settings revealing a bronchocele in the lingula (arrow).

Hochhegger B, Marchiori E, Rodrigues R, Mançano A, Jasinowodolinski D, Chate RC, Souza Jr AS, Silva AM, Sawamura M, Furnari M, Araujo-Neto C, Escuissato D, Pinetti R, Nobre LF, Warszawiak D, Szarf G, Telles GBS, Meirelles G, Santana PR, Antunes V, Capobianco J, Missie I, Souza L, Santos MK, Irion K., Duarte I, Santos R, Pinto E, Penha D

**Figure S4.** Axial CT scans with lung (A) and mediastinal window (B) settings revealing a broncholith within a segmental bronchus of the right lower pulmonary lobe (arrow).
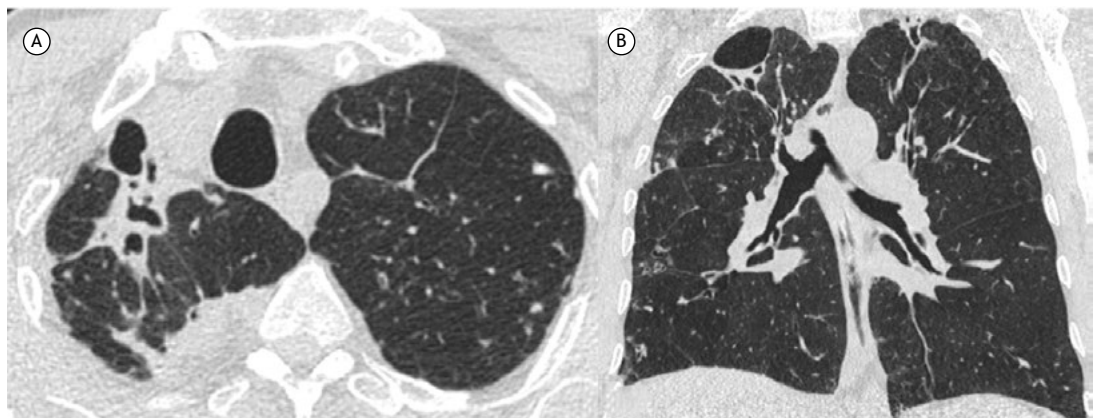


**Figure S5.** Axial CT scans with lung window settings of a male patient with multidrug-resistant tuberculosis and pulmonary fibrosis. In A, bronchiolectasis in the peripheral lung regions (arrows), in addition to centrilobular micronodules (dashed arrows) suggestive of dilated bronchioles with luminal content. In B, bronchiolectasis with thickened walls (arrows).
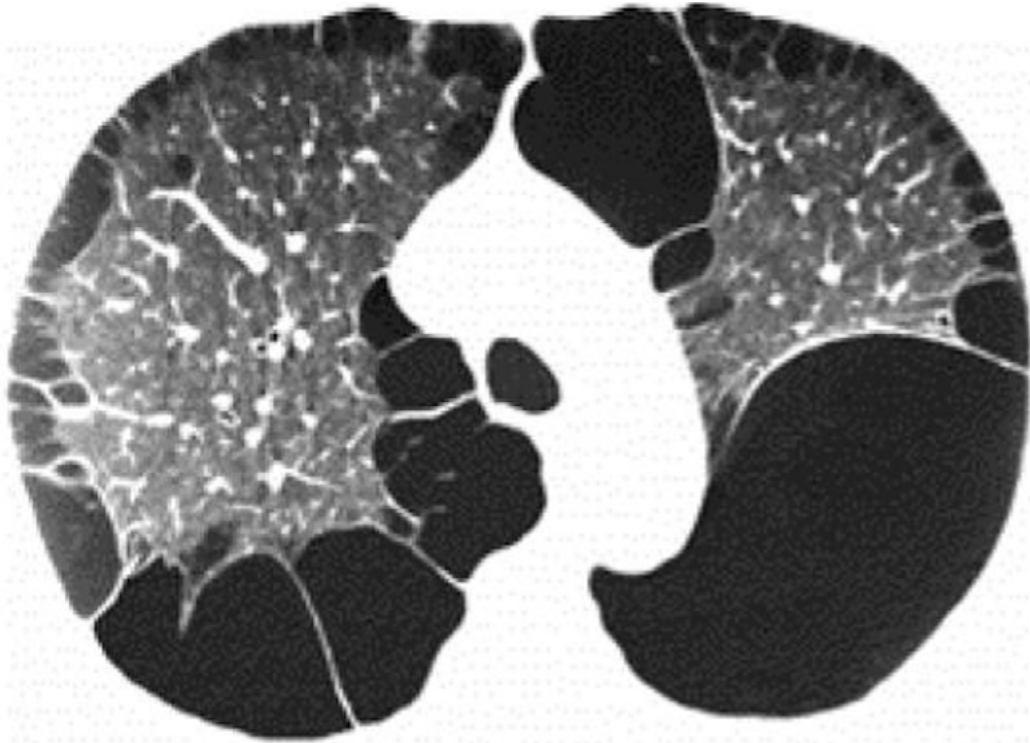
**Figure S6.** Axial CT scans with lung window settings showing traction bronchiectasis (arrow in A) and traction bronchiolectasis (arrow in B), associated with areas of lung parenchymal fibrosis.
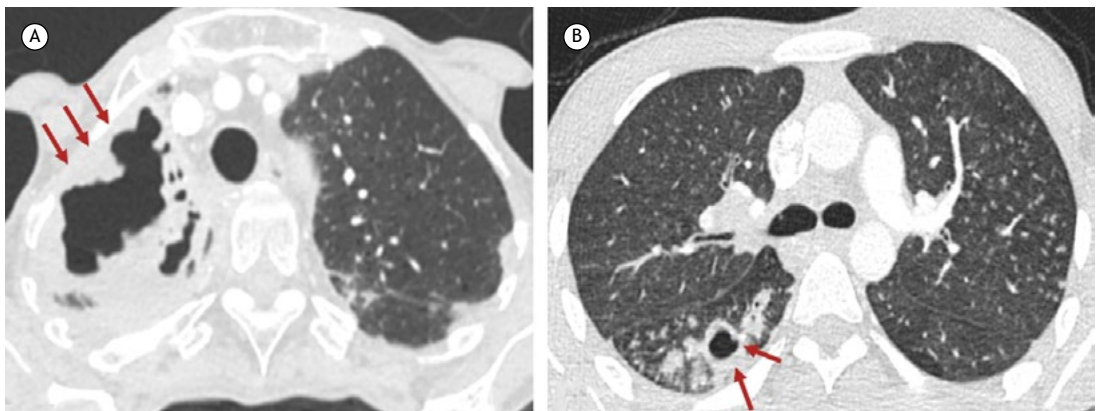


**Figure S7.** Axial CT scans with lung window settings. In A, a large fungal cavity occupying the right upper lobe (arrows). In B, a small cavity in the upper segment of the right lower lobe with several surrounding centrilobular nodules in a patient with pulmonary tuberculosis (arrows).



**Figure S8.** Axial (A) and coronal (B) CT scans with lung window settings revealing distortion of the lung parenchyma in the upper lobes, accompanied by right apical fibrosis, emphysematous bulla, and cylindrical bronchiectasis.

Hochhegger B, Marchiori E, Rodrigues R, Mançano A, Jasinowodolinski D, Chate RC, Souza Jr AS, Silva AM, Sawamura M, Furnari M, Araujo-Neto C, Escuissato D, Pinetti R, Nobre LF, Warszawiak D, Szarf G, Telles GBS, Meirelles G, Santana PR, Antunes V, Capobianco J, Missie I, Souza L, Santos MK, Irion K., Duarte I, Santos R, Pinto E, Penha D

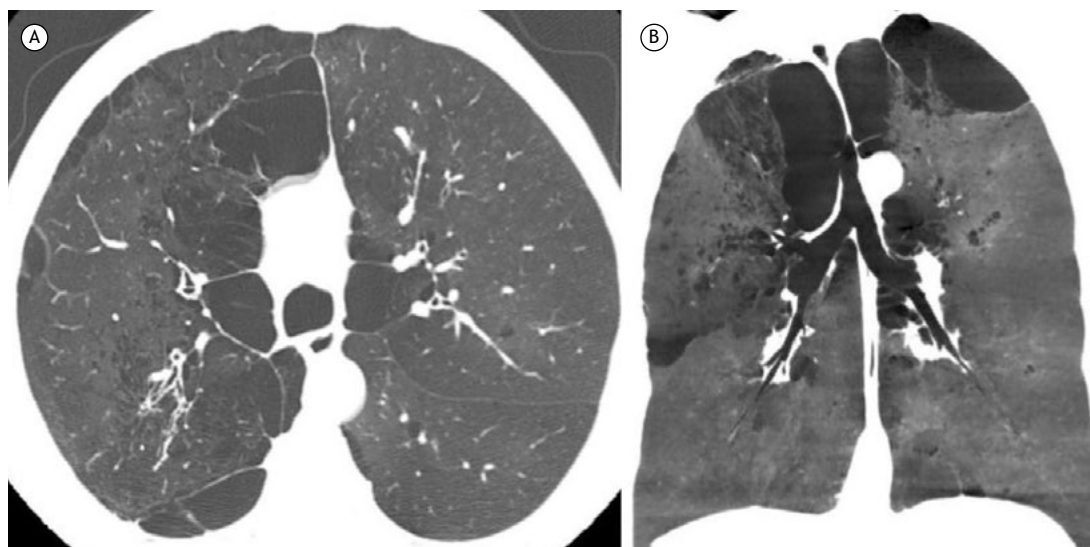**Figure S9.** An axial CT scan with lung window settings revealing severe bullous emphysema and bilateral paraseptal emphysema.
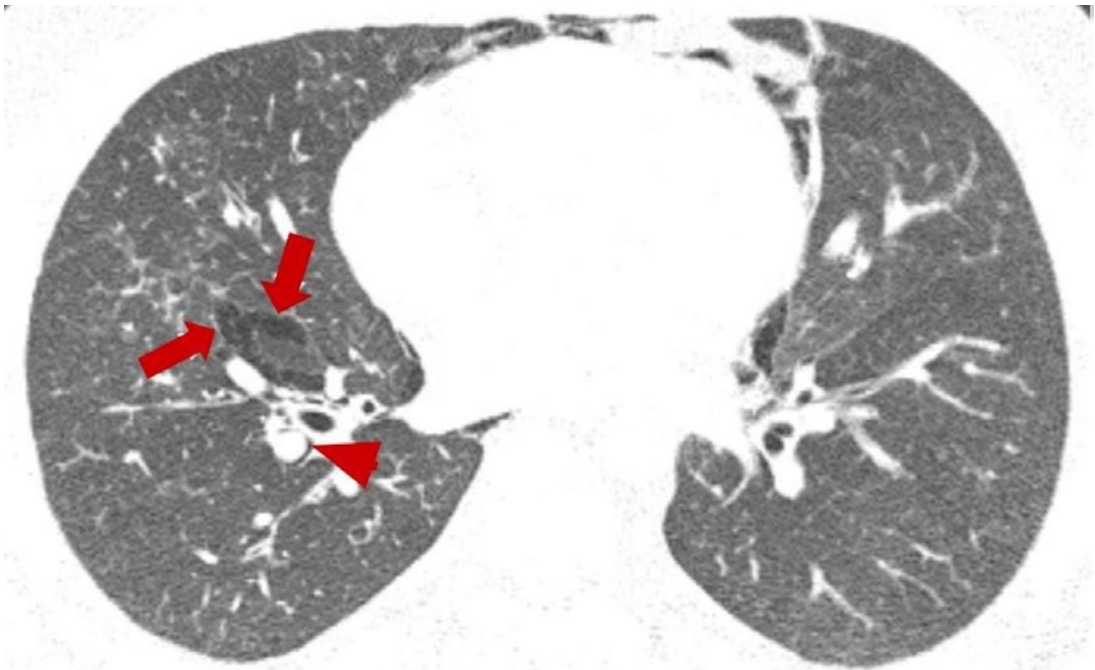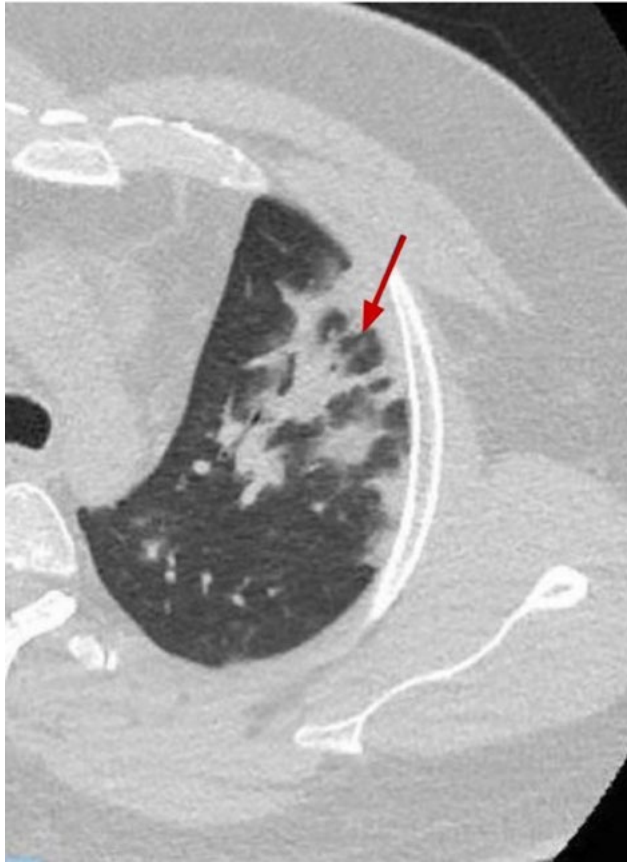


**Figure S10.** An axial CT scan with lung window settings showing, at the level of the pulmonary veins, small collections of air in a subpleural (arrows) and peribronchovascular (arrowhead) situation in the right lower lobe. There are also signs of pneumomediastinum.
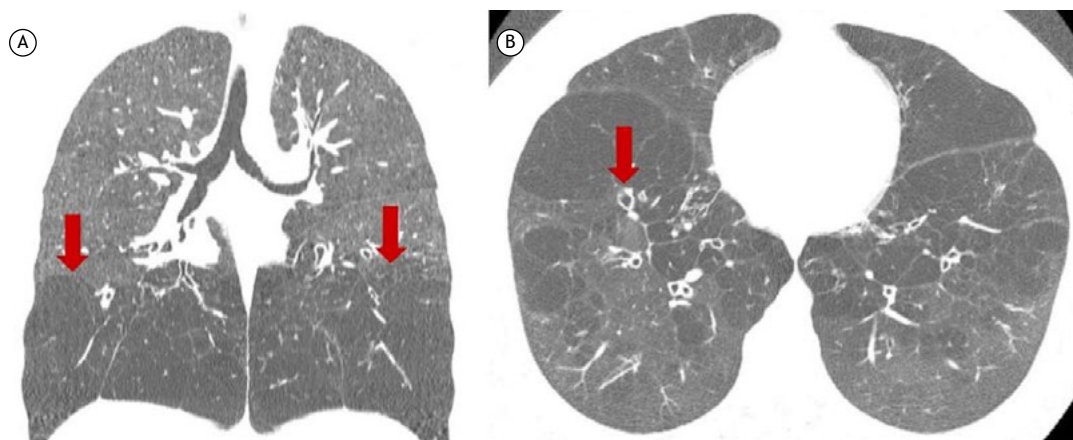
**Figure S11.** Axial CT scans with lung window settings of a male patient with alpha-1 antitrypsin deficiency. In A, a coronal scan showing areas of symmetric decrease in attenuation of the lung parenchyma and in vessel calibers at the lung bases (arrows). In B, a CT scan showing bronchiectasis (arrows).



**Figure S12.** CT scans with lung window settings. In A, an axial CT scan showing paraseptal emphysema in the upper pulmonary lobes. In B, coronal minimum-intensity projection reconstruction demonstrating subpleural cystic formations and bullae predominantly in the upper lobes, all of which being related to the paraseptal emphysema. There are also signs of centrilobular emphysema.

Hochhegger B, Marchiori E, Rodrigues R, Mançano A, Jasinowodolinski D, Chate RC, Souza Jr AS, Silva AM, Sawamura M, Furnari M, Araujo-Neto C, Escuissato D, Pinetti R, Nobre LF, Warszawiak D, Szarf G, Telles GBS, Meirelles G, Santana PR, Antunes V, Capobianco J, Missie I, Souza L, Santos MK, Irion K., Duarte I, Santos R, Pinto E, Penha D
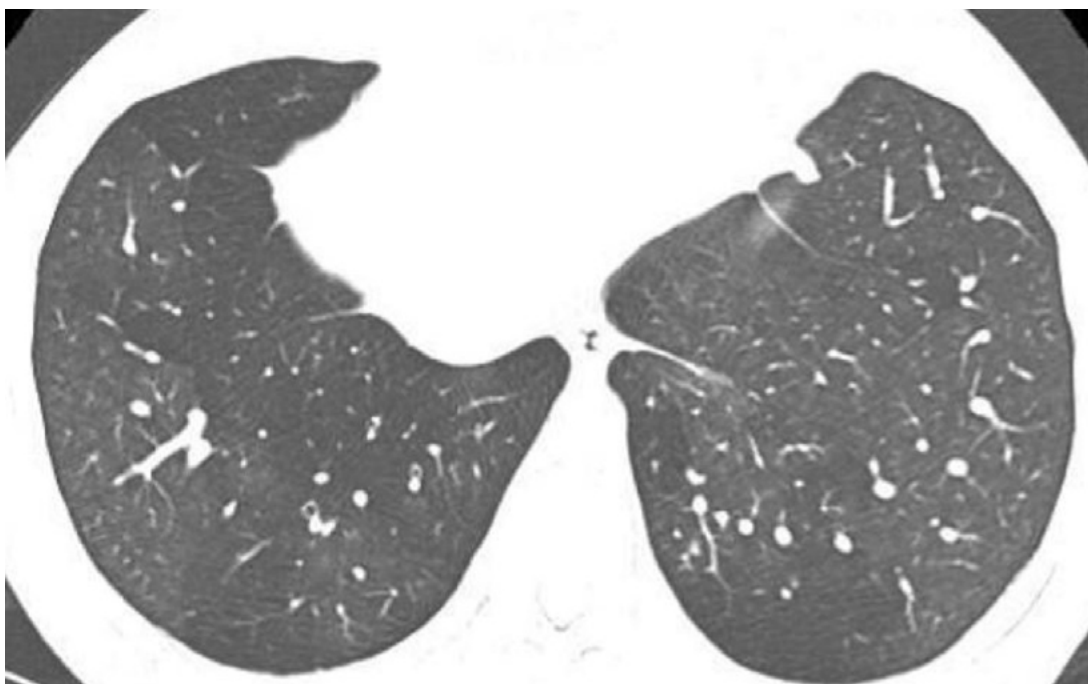
**Figure S13.** An axial CT scan with lung window settings showing consolidation in the left upper lobe, containing a focus of preserved airspace (arrow).
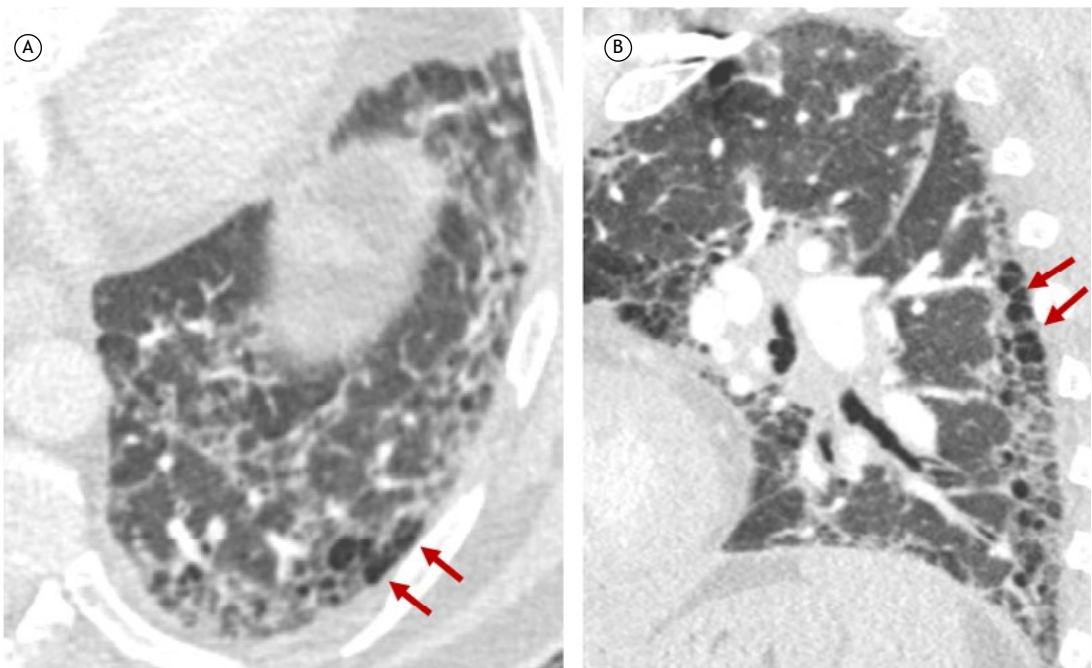


**Figure S14.** Sagittal CT scans with lung window settings revealing diffuse interlobular septal thickening, forming polygonal arcades (arrows).
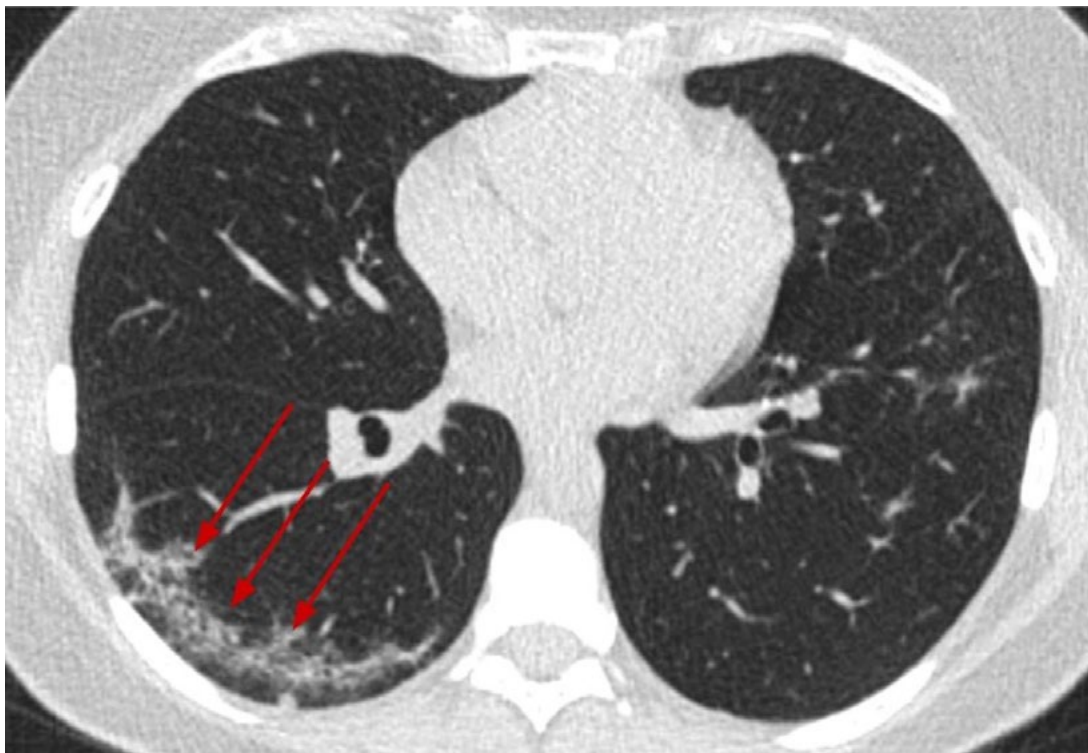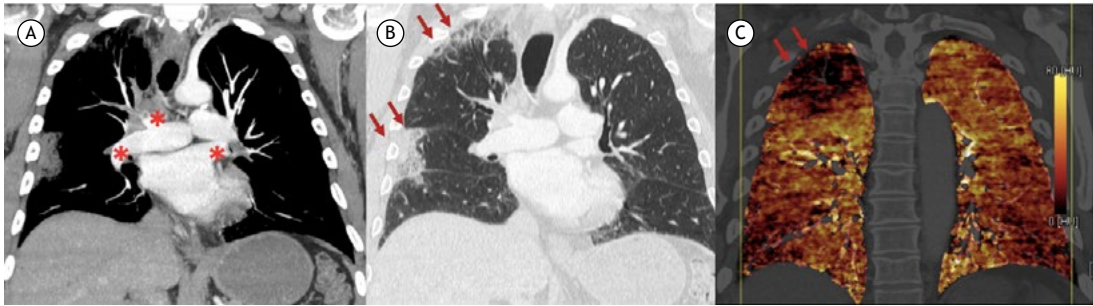
**Figure S15.** An axial CT scan with lung window settings revealing a subpleural curvilinear line (arrows) in a patient with SARS-CoV-2 infection (COVID-19).
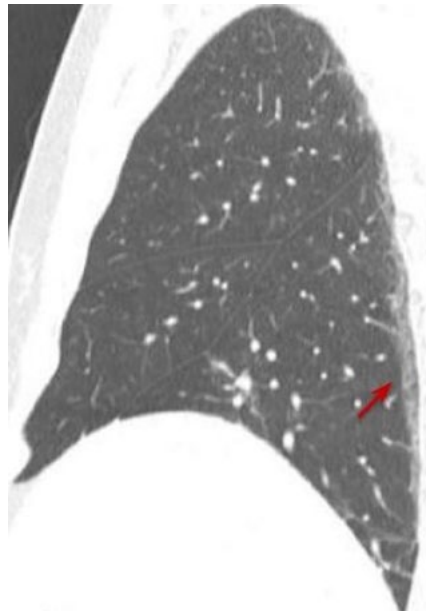


**Figure S16.** An axial CT scan with lung window settings revealing regional and bilateral areas of oligemia, more extensive on the right.

Hochhegger B, Marchiori E, Rodrigues R, Mançano A, Jasinowodolinski D, Chate RC, Souza Jr AS, Silva AM, Sawamura M, Furnari M, Araujo-Neto C, Escuissato D, Pinetti R, Nobre LF, Warszawiak D, Szarf G, Telles GBS, Meirelles G, Santana PR, Antunes V, Capobianco J, Missie I, Souza L, Santos MK, Irion K., Duarte I, Santos R, Pinto E, Penha D
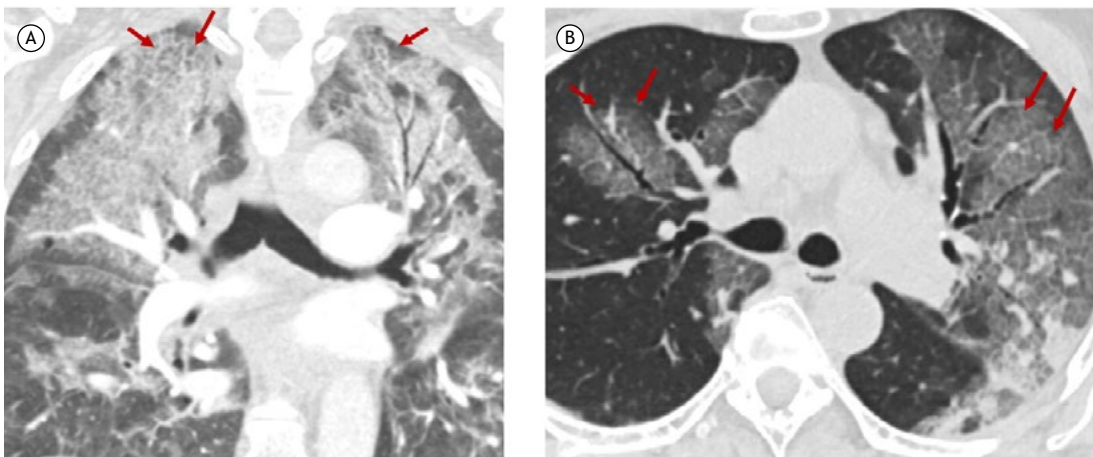
**Figure S17.** Coronal CT scans of a male patient with bilateral acute pulmonary thromboembolism. In A, a scan with mediastinal window setting showing the right upper lobe artery and segmental arteries of the middle lobe, right lower lobe (asterisks), and left lower lobe. In B, a scan with lung window settings showing peripheral right pulmonary infarcts in the territories of the affected arteries, which appear as focal ground-glass opacities (arrows). In C, a dual-energy perfusion map confirming the perfusion defects resulting from the bilateral pulmonary thromboembolism, with a significant perfusion defect in the right upper lobe (arrows).



**Figure S18.** A sagittal CT scan with lung window settings showing a dependent opacity in the posterior region of the right lower lobe (arrow).



**Figure S19.** In A, a coronal CT scan with lung window settings of a male patient with respiratory infection with *Pneumocystis carinii*, showing bilateral areas of crazy paving in the upper lobes, sparing the subpleural regions (arrows). In B, an axial CT scan of a male patient withSARS-CoV-2 infection, demonstrating several areas of ground-glass attenuation with superimposed interlobular septal thickening, corresponding to the crazy-paving pattern (arrows).
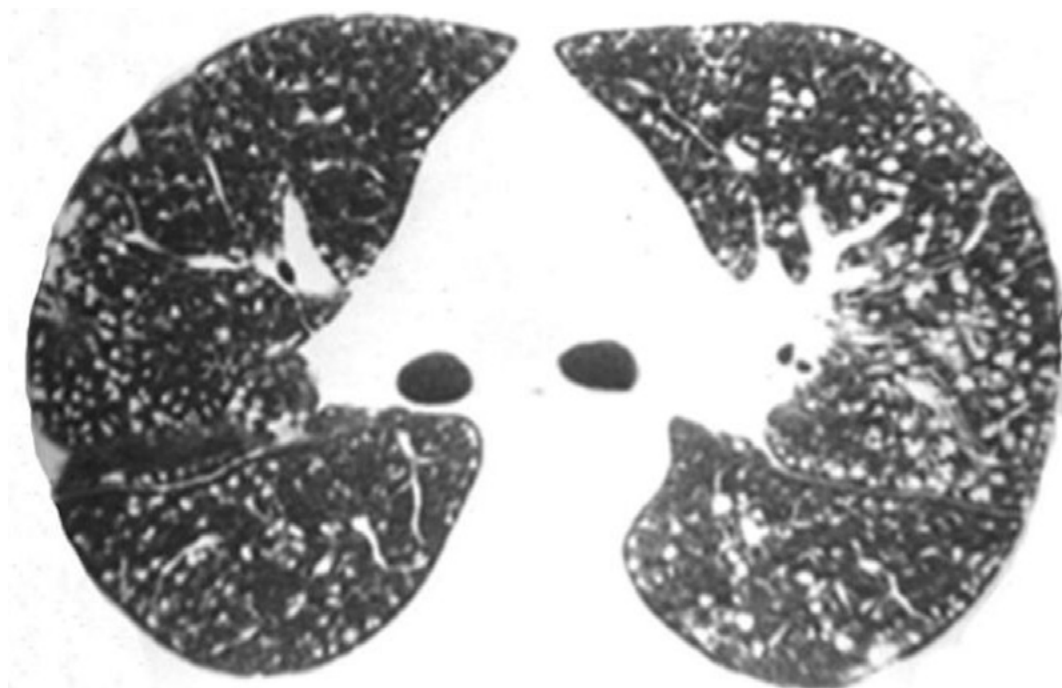
**Figure S20.** An axial CT scan with lung window settings showing, in the upper lobes, small soft-tissue density nodules that are homogeneously distributed throughout the lungs but not touching the peripheral pleural surfaces or fissures.
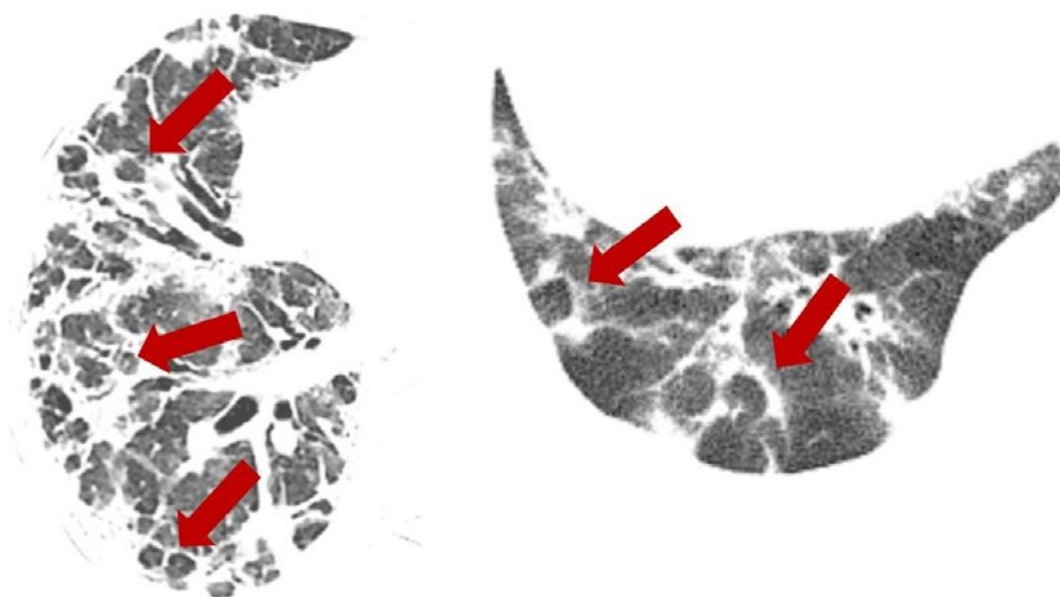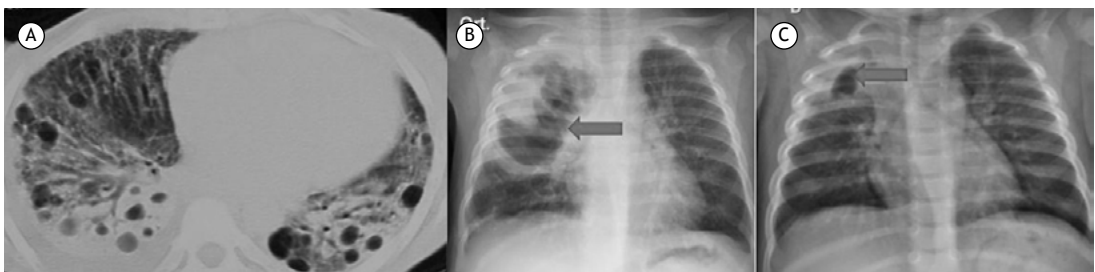


**Figure S21.** Axial CT scans with lung window settings showing the perilobular pattern, with perilobular opacities and perilobular thickening (arrows).

Hochhegger B, Marchiori E, Rodrigues R, Mançano A, Jasinowodolinski D, Chate RC, Souza Jr AS, Silva AM, Sawamura M, Furnari M, Araujo-Neto C, Escuissato D, Pinetti R, Nobre LF, Warszawiak D, Szarf G, Telles GBS, Meirelles G, Santana PR, Antunes V, Capobianco J, Missie I, Souza L, Santos MK, Irion K., Duarte I, Santos R, Pinto E, Penha D

**Figure S22.** In A, an X-ray of a male patient with pulmonary fibrosis, showing bilateral peripheral reticulation. In B, an axial CT scan with lung window settings of a male patient with pulmonary fibrosis, showing a typical peripheral reticular pattern.
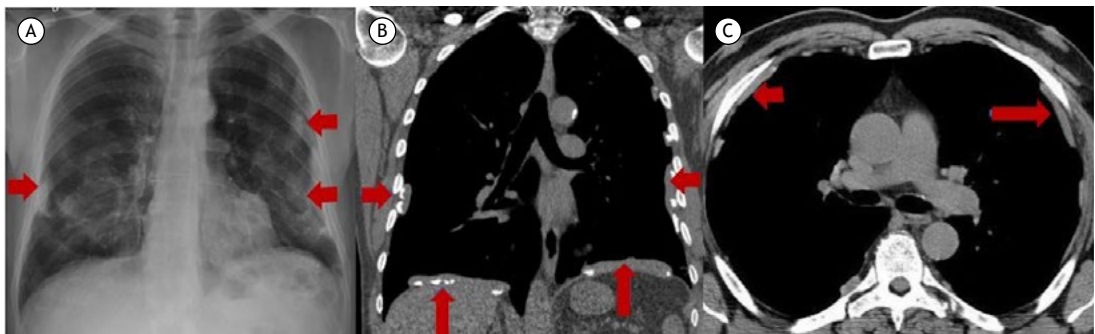


**Figure S23.** In A, an X-ray of a male patient with asbestos exposure showing multiple bilateral calcified plaques seen as dense linear structures in the periphery (arrows). In B, a coronal CT scan with mediastinal window settings revealing plaques (arrows) that are more evident on coronal than on axial images. In C, an axial CT scan with mediastinal window settings showing plaques adjacent to the hemidiaphragms (arrows), characteristic of asbestos exposure.
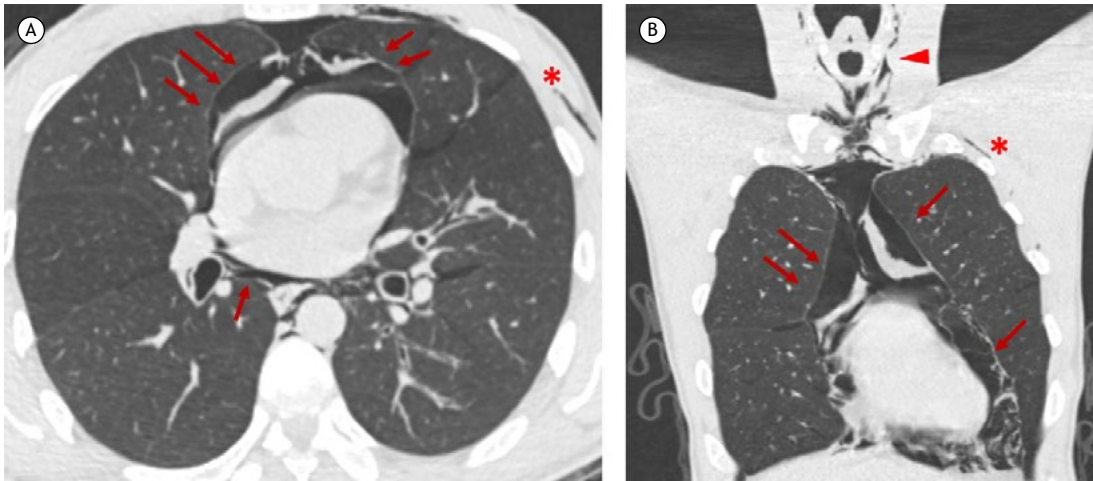


**Figure S24.** In A, an axial CT scan with lung window settings showing bilateral pneumonia with pneumatoceles. In B, an X-ray of a 9-month-old infant with pneumonia in the right upper lobe, showing a giant pneumatocele (arrow). In C, a follow-up X-ray performed three weeks later confirming the favorable outcome after antibiotic therapy (arrow).
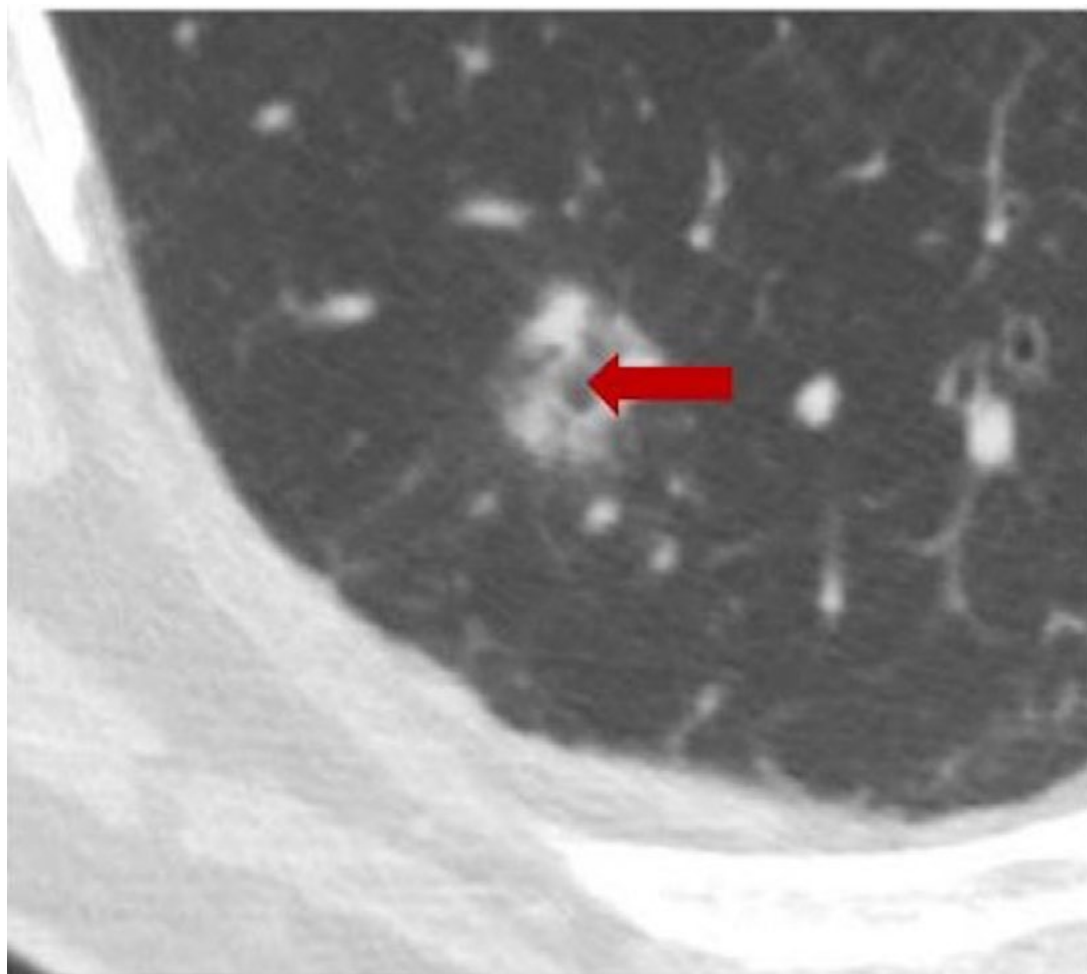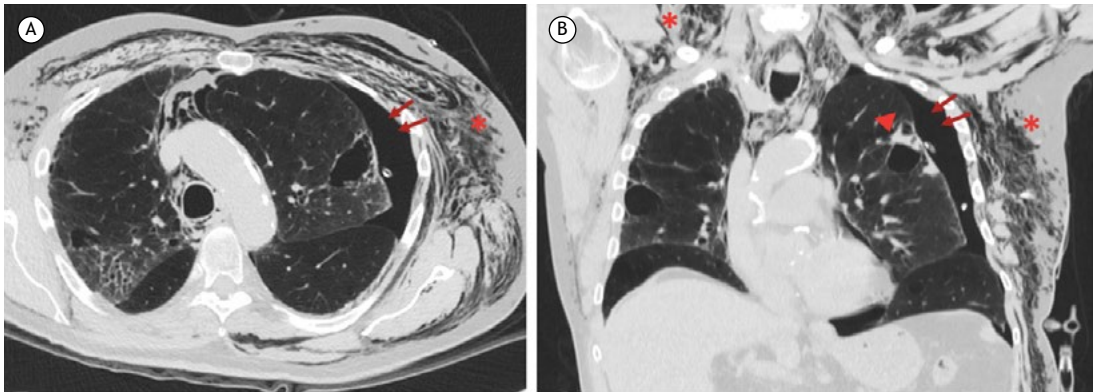
**Figure S25.** An axial CT scan with lung window settings showing a subsolid nodule containing a pseudocavity (arrow) in the right lower lobe. Pathological examination revealed it to be an adenocarcinoma.



**Figure S26.** Axial CT scans with lung window settings of a male patient with cystic lung adenocarcinoma. In A, initial screening image showing a 5-mm nodule (arrows) on the anterior wall of the cyst (asterisk) in the right lower lobe. In B, a follow-up CT scan showing nodule growth to 7 mm. In C, a CT scan performed 24 months after the initial screening study, confirming significant nodule growth to 12 mm. Pathological examination confirmed adenocarcinoma.

Hochhegger B, Marchiori E, Rodrigues R, Mançano A, Jasinowodolinski D, Chate RC, Souza Jr AS, Silva AM, Sawamura M, Furnari M, Araujo-Neto C, Escuissato D, Pinetti R, Nobre LF, Warszawiak D, Szarf G, Telles GBS, Meirelles G, Santana PR, Antunes V, Capobianco J, Missie I, Souza L, Santos MK, Irion K., Duarte I, Santos R, Pinto E, Penha D

**Figure S27.** Axial (A) and coronal (B) CT scans with lung window settings showing the presence of air in the mediastinal compartment, with dissection of gas along the pericardium and pleura (arrows), in addition to the presence of air in the posterior mediastinum, with dissection of gas to the neck spaces (arrowhead). Note also the presence of subcutaneous emphysema (asterisk).
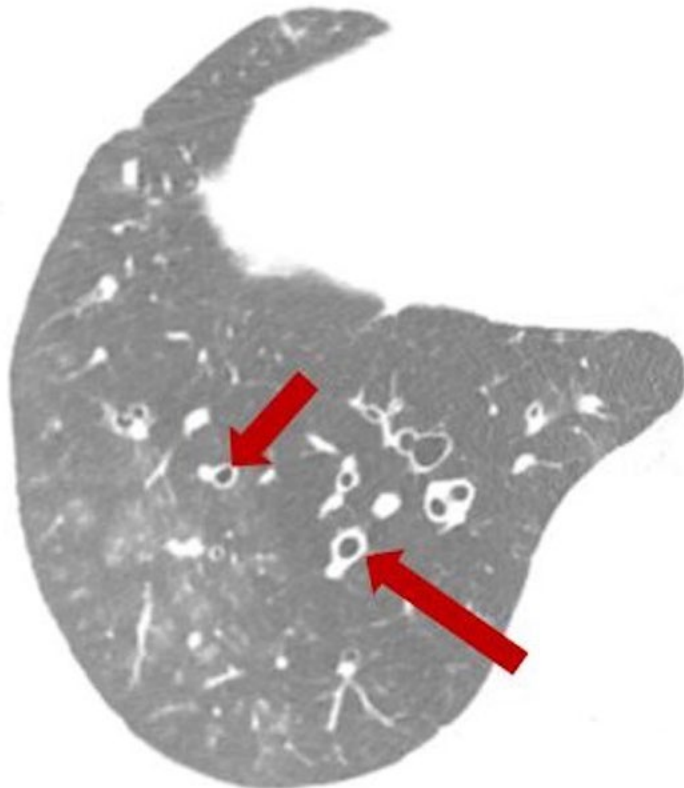


**Figure S28.** Axial (A) and coronal (B) CT scans with lung window settings showing the presence of air in the pleural cavity (arrows) after percutaneous biopsy of carcinoma associated with a cystic space in the left upper lobe (arrowhead). Note also the presence of subcutaneous emphysema (asterisk) with dissection of anterior and posterior chest wall muscles.
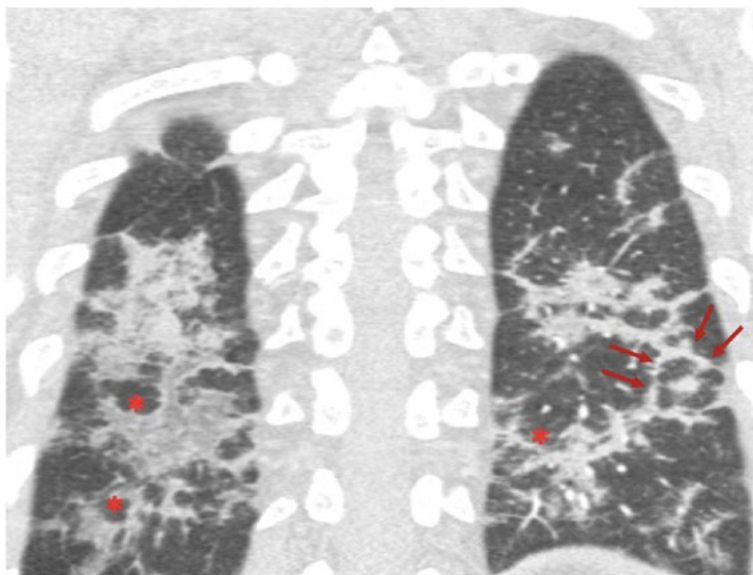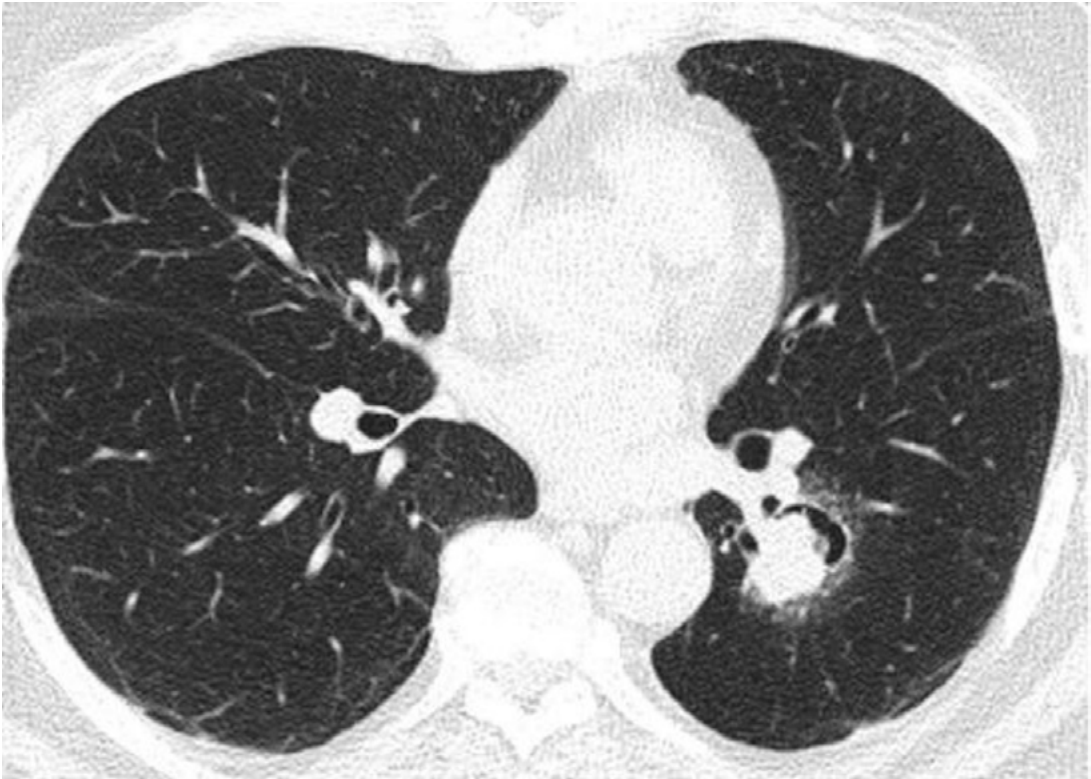


**Figure S29.** A coronal CT scan with lung window settings showing extensive bilateral organizing pneumonia with a perilobular distribution (asterisk) and with a target sign in the left lower lobe (arrows), characterized by peripheral opacity and a central nodular area.
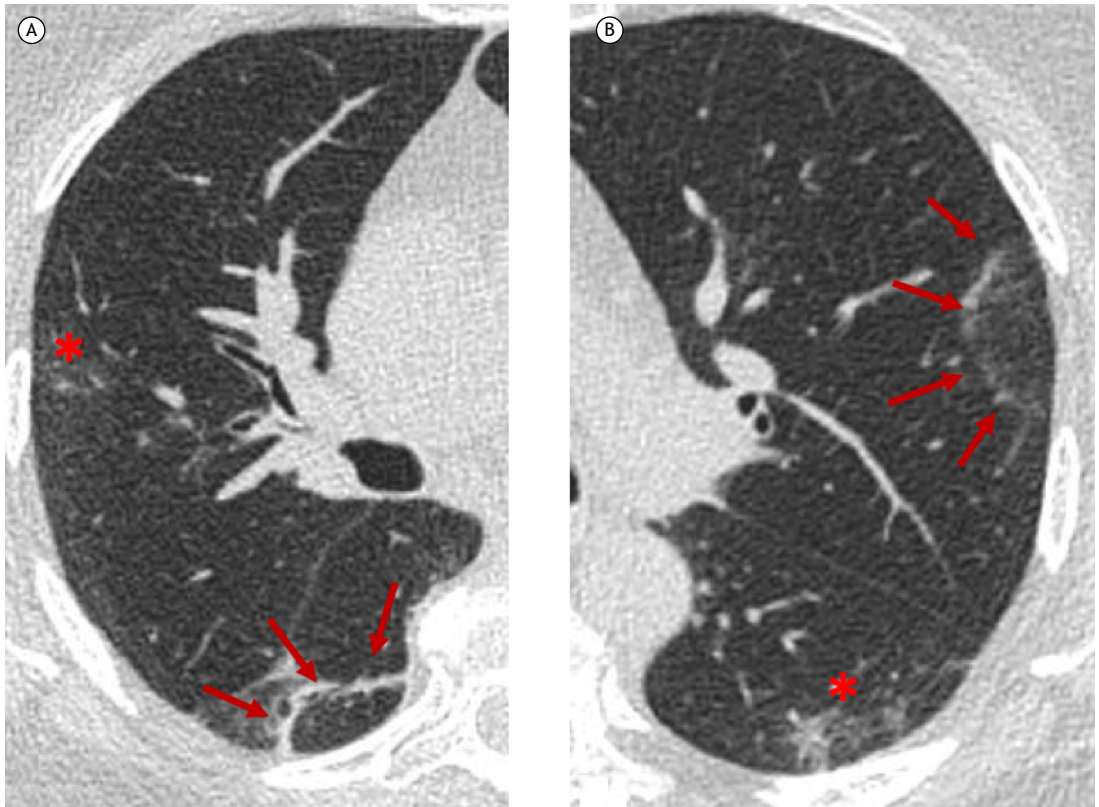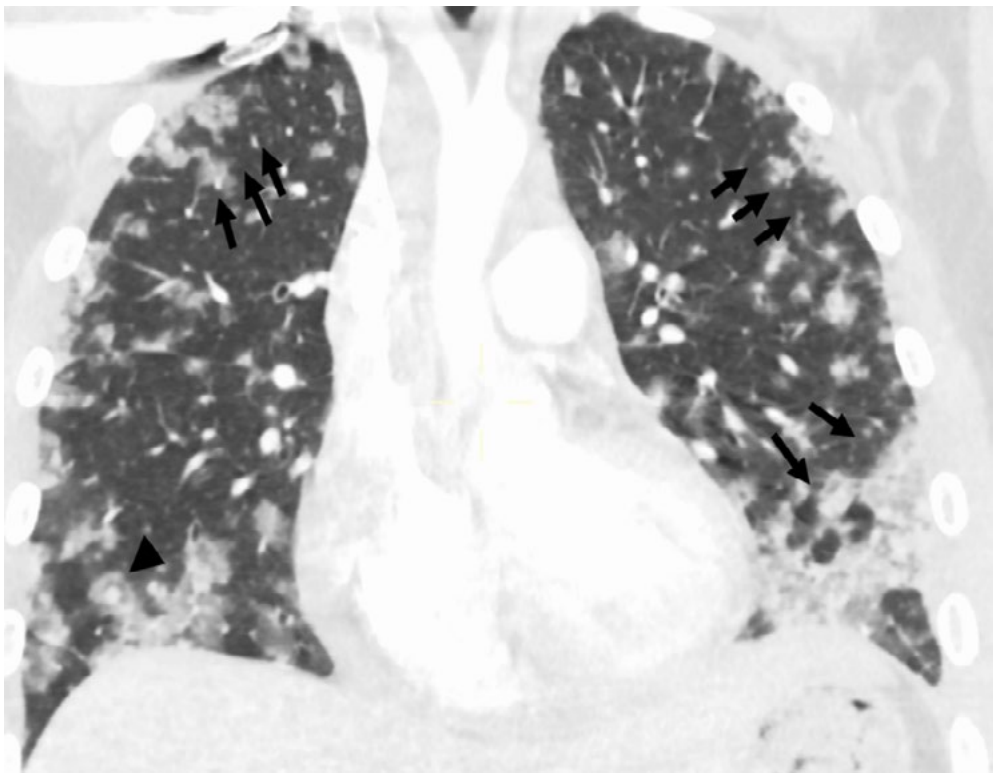
**Figure S30.** Axial CT scans with lung window settings of two male patients with COVID-19, showing an arch-shaped linear opacity around the secondary pulmonary lobule, that is, the arch sign (arrows). Note also some focal ground-glass areas (asterisks).
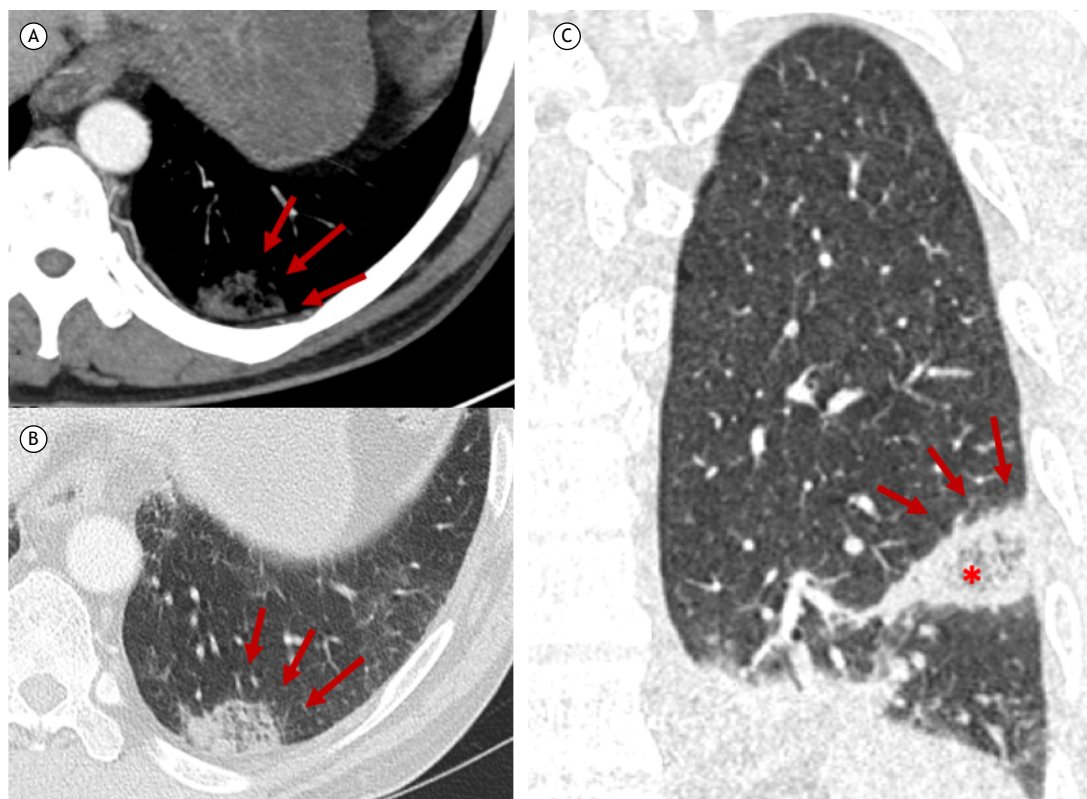


**Figure S31.** An axial CT scan with lung window settings showing the signet ring sign (arrow).

Hochhegger B, Marchiori E, Rodrigues R, Mançano A, Jasinowodolinski D, Chate RC, Souza Jr AS, Silva AM, Sawamura M, Furnari M, Araujo-Neto C, Escuissato D, Pinetti R, Nobre LF, Warszawiak D, Szarf G, Telles GBS, Meirelles G, Santana PR, Antunes V, Capobianco J, Missie I, Souza L, Santos MK, Irion K., Duarte I, Santos R, Pinto E, Penha D

**Figure S32.** An axial CT scan with lung window settings showing the air crescent sign in a male patient with lung cancer in the left lower lobe.



**Figure S33.** An axial CT scan with lung window settings of a male patient with cardiac angiosarcoma with lung metastasis, revealing several soft-tissue density nodules bilaterally (arrows), some of which being surrounded by a halo of ground-glass opacity (arrowhead).
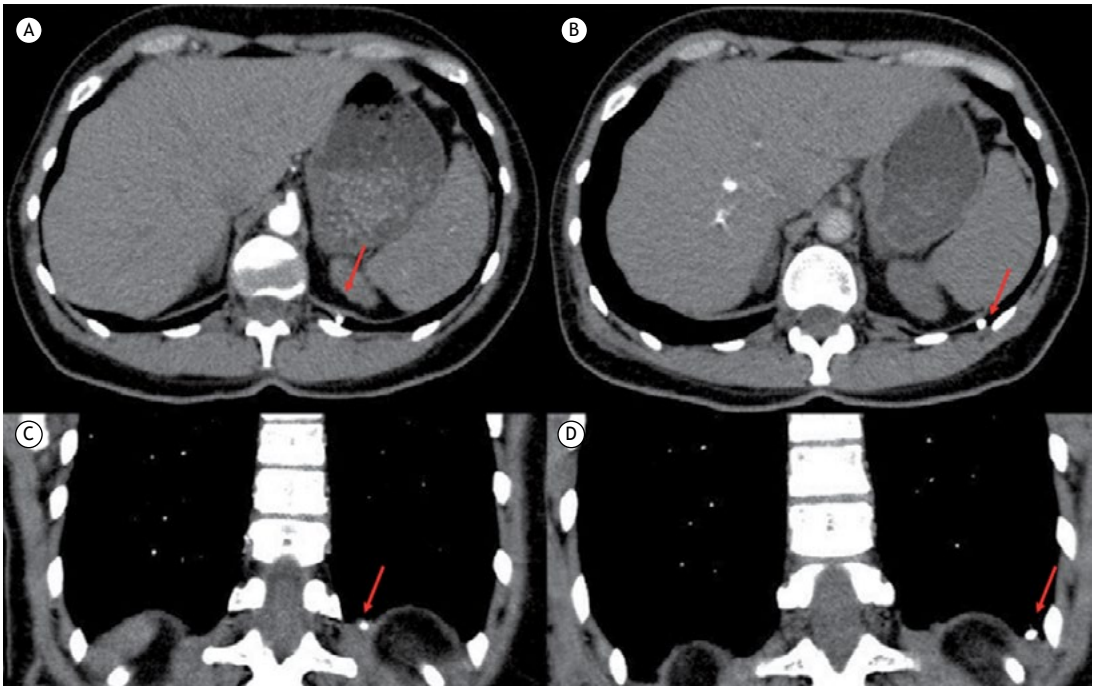
**Figure S34.** Axial (A) and coronal (B) CT scans with mediastinal window settings, and a coronal CT scan with lung window settings (C) showing the reversed halo sign, with ground-glass opacity surrounded by peripheral consolidation (arrows). Note the reticular pattern within the reversed halo sign, characteristic of peripheral pulmonary infarction (asterisk).



**Figure S35.** Axial CT scans with lung window settings showing the beaded septum sign in three patients with different diagnoses: sarcoidosis (A); esophageal carcinoma and lymphangitic carcinomatosis (B); and bronchus-associated lymphoid tissue lymphoma (C).

Hochhegger B, Marchiori E, Rodrigues R, Mançano A, Jasinowodolinski D, Chate RC, Souza Jr AS, Silva AM, Sawamura M, Furnari M, Araujo-Neto C, Escuissato D, Pinetti R, Nobre LF, Warszawiak D, Szarf G, Telles GBS, Meirelles G, Santana PR, Antunes V, Capobianco J, Missie I, Souza L, Santos MK, Irion K., Duarte I, Santos R, Pinto E, Penha D

**Figure S36.** Axial (A and B) and coronal (C and D) CT scans with mediastinal window settings of a male patient with a mobile calcified nodule (arrows) in the pleural surfaces. Note the different position of the nodule on the two axial views and on the two coronal reconstructions.

In the article "Consensus statement on thoracic radiology terminology in Portuguese used in Brazil and in Portugal", DOI number http://dx.doi.org/10.36416/1806-3756/e20200595, published in the Jornal Brasileiro de Pneumologia, 47(5):e20200595,2021, in the first page:

Where it reads:
Marcel Koeningan Santos

It should be read:
Marcel Koenigkam Santos